Proceedings of the Second International Conference on Press-in Engineering 2021, Kochi, Japan – Matsumoto et al (eds)
© 2021 Taylor & Francis Group, London, ISBN 978-1-032-10414-0

Experimental observation on the ultimate lateral capacity of vertical-batter screw pile under monotonic loading in cohesionless soil

A. Jugdernamjil & N. Yasufuku
Kyushu University, Fukuoka-shi, Japan

Y. Tani, T. Kurokawa & M. Nagata
HINODE Co., Ltd, Fukuoka-shi, Japan

ABSTRACT: 1g model experimental studies were carried out in the laboratory to evaluate vertical performance with varying angles battered pile in dense sand. Relatively rigid piles with slenderness ratios 9 and 13.5 were undertaken in a sand-filled tank under strain-controlled lateral loading. The tank dimensions were designed so that boundary effects could be minimized and earth pressure measured using transducers at the front and bottom, and rear in each case. The relative density of 90% was achieved to simulate a more precise field condition in all test cases using the tamper compaction method. In order to determine the efficiency of the ultimate bearing capacity of screw pile configurations in lateral loading, the plate and pipe pile configurations were chosen for comparison. Totally 26 experimental cases were performed, which included vertical-batter combinations. The results indicated that the load-displacement characteristic was nonlinear under lateral loading. The case of 45 degree demonstrated higher ultimate lateral resistance.

1 INTRODUCTION

In recent years, in agriculture and civil engineering, the screw pile is becoming popular in supporting foundations designated in soft ground. A screw pile is made by twisting a flat steel bar. It has a lower bending stiffness than other conventional piles because of its lower cross-section area (Figure 1). Preceding research on the bearing and pull-out capacity of the screw pile was studied by Sato et al. 2014, and Wang et al. 2018. Wang et al. 2018 found out that the optimal pitch width ratio (p/w) under a pull and pushing test is 4.5, selected in this experimental study. In this experimental test, the pitch and width of the screw model pile were taken as 72 mm and 16 mm, respectively, as shown in Figure 1. The pitch width ratio is equal with dividing pitch length by width length. As mentioned above, the screw piles and anchors are implemented in the foundation of greenhouses, solar panel farms, wind turbines, road signs, and guide rails because of their applicable axial loading and simple installation.

The present study focuses on the foundation of guide rails for protection from a vehicle accident that gives impact loading to them. The resultant lateral impact is made over lateral displacement in a single screw foundation due to less frontal and side soil resistance than a conventional pipe pile. Therefore, additional reinforcement is required for improving lateral performance. The screw shape, which has a limitation that the lateral resistance is less than a steel pipe pile even having the same diameter, caused less bending rigidity concerning the lateral direction loading.

In the literature, as a method of improving the horizontal resistance, increasing pile dimensions such as length and diameter can be mentioned. However, about a screw shape, there is a limitation in the manufacturing and installation environment. Thus, the coupled piles may be one of the improvement techniques in the lateral capacity, consisting of vertical and batter piles. In the decades, quantitative empirical and theoretical studies have been done on the lateral capacity of the conventional rigid pile such as tapered pile, belled-type pile, and steel H-pile in cohesionless soil using approaches such as analysis based on limiting equilibrium or plastic theory, analysis based on elastic theory, and nonlinear analysis. Furthermore, one of the representatives of screw type of pile is the helical pile. The theoretical and empirical studies on the helical pile can be found in the literature. However, the study on the pile made by a flat bar twisting into a screw is scarce.

The aim of this research is to observe the lateral capacity of a single screw pile by a 1-g model test and comparing it with conventional model pile types

DOI: 10.1201/9781003215226-17

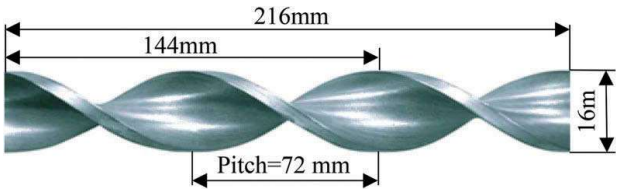

Figure 1. View of screw pile.

such as a flat bar and a pipe. Additionally, in order to find out an optimal and rational angle between the vertical and batter piles for reinforcing a single screw pile, the cases of 30, 45, and 60 degrees are performed and evaluated.

2 METHODOLOGY

2.1 *Experimental test apparatus*

A macro-scale 1g model test was performed to determine the behavior of the lateral capacity of the screw pile and its combination. Figure 2 shows the experimental test setup conducted in this study. Lateral monotonic displacement was applied to the top of the pile. Pile head displacement of 20mm was applied, and the allowable pile capacity was taken as the load corresponding to 0.2D (3.2mm) of pile head deflection (Narasimha Rao et al. 1998, Chandrasekaran et al. 2010). The lateral load was applied at the pile head as free with an eccentricity of 40mm.

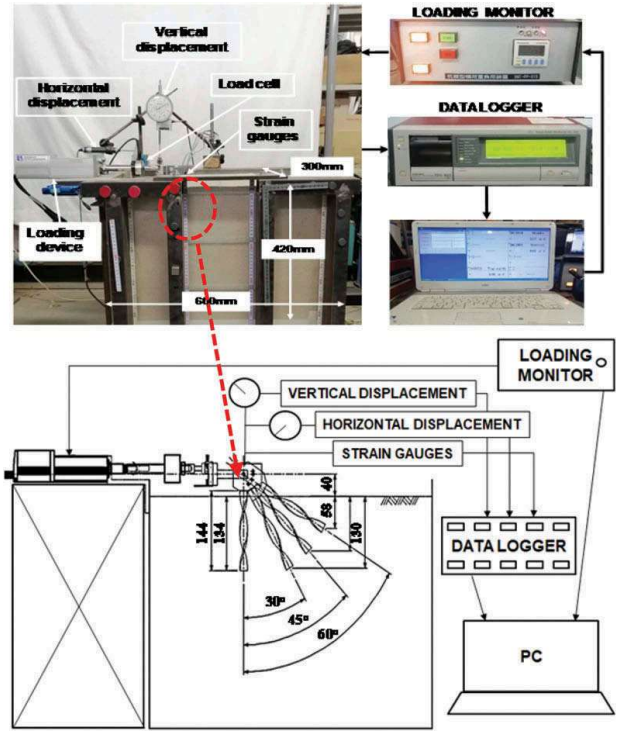

Figure 2. Schematic of experimental apparatus.

2.2 *Model pile*

Three types of model piles were tested, such as a steel screw, a flat bar, a pipe in this study for comparing lateral capacities. The screw pile was made by twisting a flat bar. The dimensions of the flat bar and a screw were the same: the thickness was 3mm, and the width was 16mm, respectively. The outer diameter of the pipe was equal to 16mm and 3mm thickness. The Young`s modulus of the used steel model piles was 2×10^{11}N m^{-2}. The scaling of the model pile was adjusted for the chamber dimension that minimized its boundary effect. Considering the influence range as five times of pile diameter (5D), the lengths of the pile were set to 144mm and 216mm. Slenderness ratios (L/D) of the model pile were 9 and 13.5, respectively.

The scaling of each dimension is shown in Table 1. Dimensions of the model pile of the pipe and the flat bar were settled the same as the model of the screw pile. The scaling of the prototype represented by the model pile was calculated using the following formula (Wood et al. 2002):

$$\frac{E_m I_m}{E_p I_p} = \frac{1}{F^{4.5}} \quad (1)$$

where F = scale factor: $E_m I_m$=flexural rigidity of model pile; and $E_p I_p$ = flexural rigidity of prototype. For an assumed cast iron prototype screw pile of diameter 220mm, the scaling factor is estimated at 10.

A pile in cohesionless soil can be considered to be rigid for practical purposes if the following condition is satisfied:

$$\frac{L}{T} \leq 2 \quad (2)$$

In which $T = \sqrt[5]{\frac{EI}{n}}$

Table 1. Properties of model piles.

	Model		Prototype	
Material	Steel		Cast Iron	
E [GPa]	200		170	
I_x [m^4]	3.60E-11		1.34E-06	
I_y [m^4]	1.02E-09		3.81E-05	
EI_x [N·m_2]	0.01		227.68	
EI_y [N·m2]	0.20		6476.34	
Length [m]	0.14	0.216	2	3
Diameter [m]	0.016		0.22	
Thickness [m]	0.003		0.04	
Scale factor [x axis]	1		10	
Scale factor [y axis]	1		10	

L = length of the pile; EI = flexural rigidity; and n = constant of horizontal subgrade reaction.

Figure 3 illustrates a comparison of the pile flexural rigidity with a depth between a screw, a flat bar, and a pipe. The moment of inertia of the screw varied along with the actual depth. For simplification, a four-point bending test was performed in screw piles for obtaining moment of inertia, which was close to 15 degrees tilted flat bar (I=20.4 Pa•m^4) using the following equation (2):

$$I = \frac{bh \cdot \left(h^2 \cdot cos^2\theta + b^2 \cdot sin^2\theta\right)}{12} \qquad (2)$$

Where θ is the angle of a tilted flat bar with the axis.

2.3 *Soil setup*

Tests were conducted in a rectangular chamber; width 30cm, length 60cm, height 42cm, respectively. The sand used in the experiment was dried at the room temperature with a uniformity coefficient of 1.76 and a specific gravity of 2.63. Figure 4 shows the grain size distribution of soil samples used in this study. The height of the chamber was divided into 12 layers of thickness. For the required density of soil corresponding to 90% relative density, the weight of soil to be filled in each layer was calculated and poured into the chamber. The wooden stick was used to compact for satisfying uniformity all over the soil medium. This preparation method was approximate; however, it was conducted with as much care as possible. Relative density may be varied by 3% (Dr = 87-90%). Triaxial tests gave a friction angle of 42° at a dense density, γ = 15.2kN/m^3.

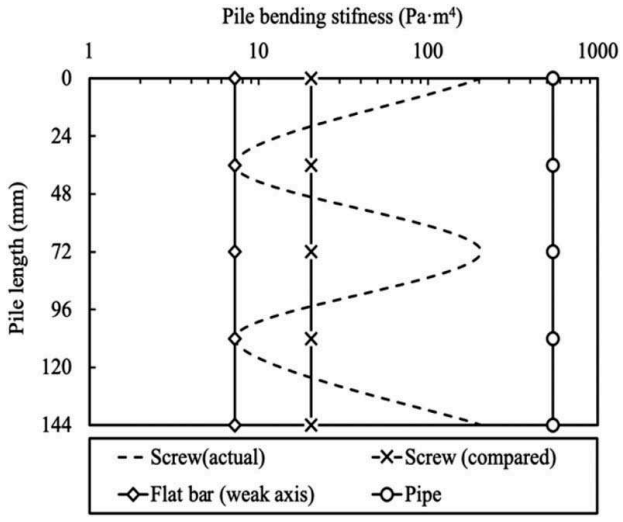

Figure 3. Variation of pile bending stiffness with depth.

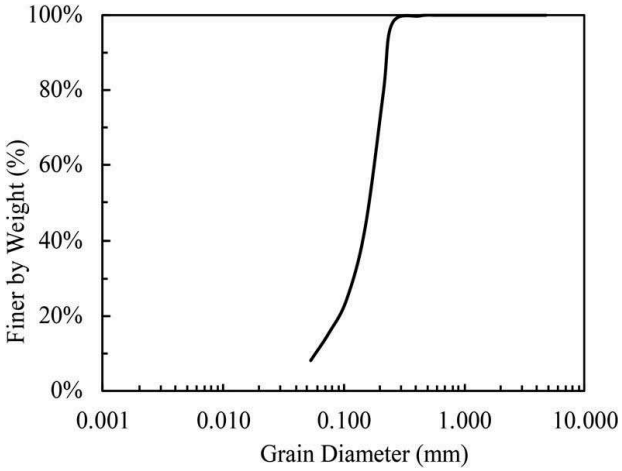

Figure 4. Grain size distribution curve of K7.

Initially, the sand was filled up to the tip of the model pile, and after that model pile was kept in its position, the sand was filled again. After running the test, the sand medium was removed, and model piles were detached. Lateral load on the pile was applied with servo cylinder and was measured with load cell attached to the cylinder head with loading rate 0.01mm/sec. A data

Overall, 26 cases were conducted with dense sand (Table 3).

In order to obtain bending moment through pile length, the strain gauges were attached to both front and rear sides, as shown in Figure 5. Cables of strain gauges were managed by bonding on the pile surface. The strain along the pile was measured with the use of a strain gauge, and the corresponding bending moments were calculated. Totally, 16ea strain gauges were attached to the coupled short model pile and 24ea strain gauges for the longer model pile using a proper bond. The strain gauge model FLA-200-3 made by Tokyo Measuring Laboratory was conducted in this experimental study. Each strain gauge was connected to the data logger and recorded during lateral loading.

Table 2. Index properties of soil medium.

Properties	Value
Specific gravity, Gs	2.63
Maximum dry density, ρ_{max}	1.56 g/cm^3
Minimum dry density, ρ_{min}	1.19 g/cm^3
Coefficient of uniformity, U_c	1.76
Median diameter, D_{50}	0.17 mm
Relative density, Dr=90%	1.53 g/cm^3
Internal friction angle, °	42°

Table 3. Experimental test conditions.

Test ID	Batter angle (°)	No. Pitch	L/D	y [mm]
S-Screw144	0	2	9	3.2
30-Screw144	30	2	9	3.2
45-Screw144	45	2	9	3.2
60-Screw144	60	2	9	3.2
S-Pipe144	0	-	9	3.2
30-Pipe 144	30	-	9	3.2
45-Pipe 144	45	-	9	3.2
60-Pipe 144	60	-	9	3.2
S-Flatbar144	0	-	9	3.2
30-Flatbar144	30	-	9	3.2
45-Flatbar 144	45	-	9	3.2
60-Flatbar 144	60	-	9	3.2
S-Screw216	0	3	13.5	3.2
30-Screw216	30	3	13.5	3.2
45-Screw216	45	3	13.5	3.2
60-Screw216	60	3	13.5	3.2
S- Pipe216	0	-	13.5	3.2
30-Pipe216	30	-	13.5	3.2
45- Pipe216	45	-	13.5	3.2
60- Pipe216	60	-	13.5	3.2
S-Flatbar216	0	-	13.5	3.2
30-Flatbar216	30	-	13.5	3.2
45-Flatbar216	45	-	13.5	3.2
60-Flatbar216	60	-	13.5	3.2
45-Screw144-216	45	2;3	-	3.2
45-Screw216-144	45	3;2	-	3.2

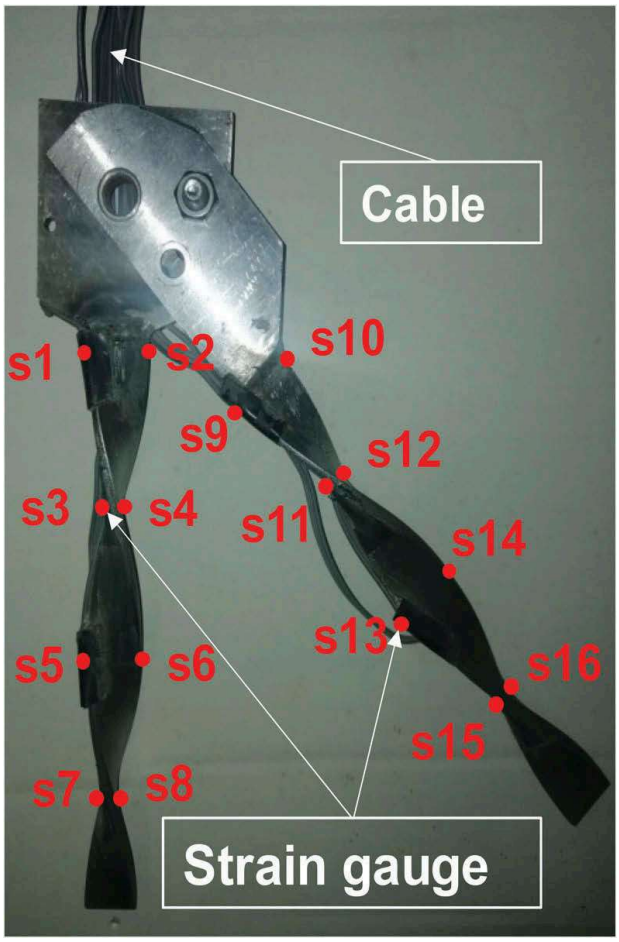

Figure 5. Strain gauge attachment.

3 RESULTS AND DISCUSSIONS

3.1 *Bending moment of the model pile*

The yield stress at 10N and 30N was selected in respective shorter and longer model piles for collecting strain values. In order to measure precise bending moment along with the pile, the pure bending strain value was calculated in respective model piles considering front and rear strain data. The bending moment along the length of the pile was calculated using the following equation:

$$M_y = S \times \sigma_y \quad (3)$$

Where S = section modulus of the model pile, σ_y = yield stress.

Figure 6-7 illustrates the variation of bending moment with the depth of the screw, the flat bar, and the pipe on single and coupled piles. The left-hand figures describe the vertical pile bending moment. Meanwhile, right-hand ones describe the bending moment of the batter pile (or reinforcement pile).

Bending moment in single piles is shown relatively higher than vertical pile in coupled piles. The trend of the curves showed a similar pattern in the screw, flat bar, and pipe. Results indicated a rather small strain along with the pile, such as less than 1kNmm. Bending moments in a single pile of 216 mm cases were reduced much comparing with the 144 mm after reinforcing by batter pile. Bending moments in 216 mm shows the amount that less than 4kNmm in vertical piles. The maximum bending moments in the configurations were shown in the same depth (d = 62 mm) aside from the case of pipe pile in 216 mm (d = 98 mm).

Based on the bending moment results, after reinforcement, the bending moments were transferred from the vertical piles to batter piles effectively.

3.2 *The ultimate lateral capacity of piles*

Nonlinear load-deflection curves of the model pile were measured from the monotonic lateral load test shown in Figure 8. In the literature, various criteria have been proposed to consider the ultimate lateral

capacity of model piles from the lateral load-deflection curve. Meyerhof et al. (1981), Rao & Prasad (1993), Georgiadis & Georgiadis (2010), Lee et al. (2010) suggested that the ultimate pile capacity

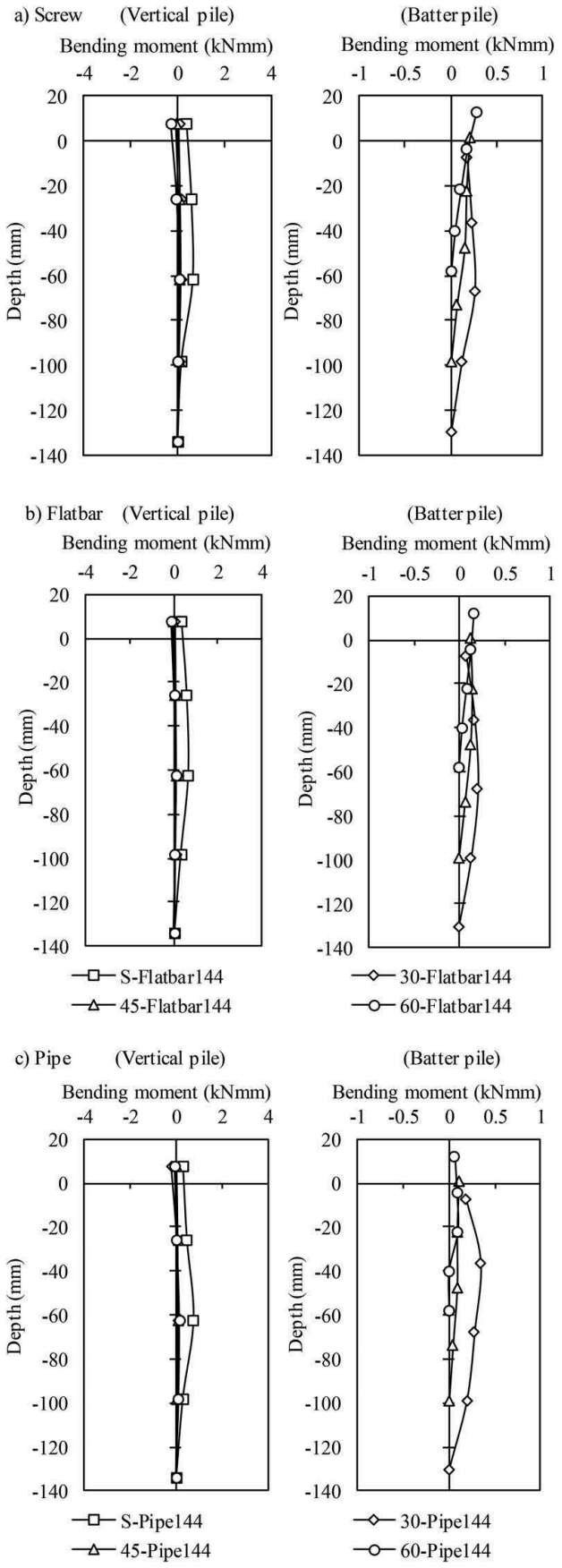

Figure 6. Variation of bending moment with a depth of 144mm model pile a) Screw b) Flat bar c) Pipe.

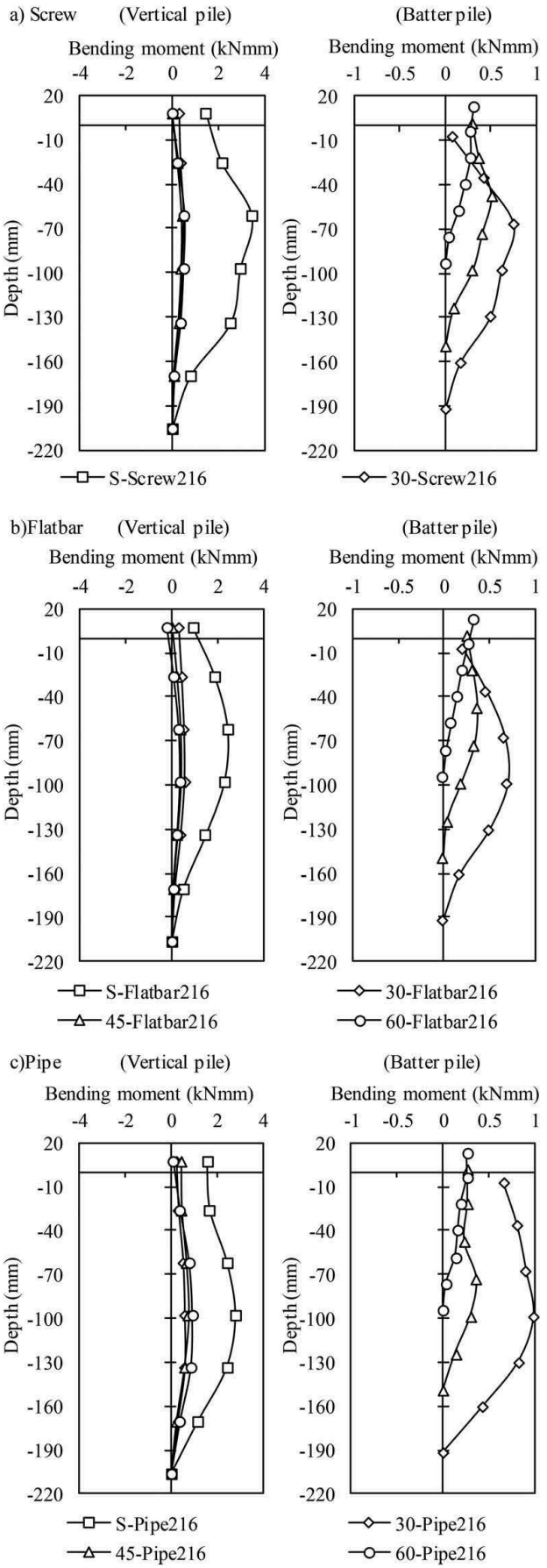

Figure 7. Variation of bending moment with a depth of 216mm model pile a) Screw b) Flat bar c) Pipe.

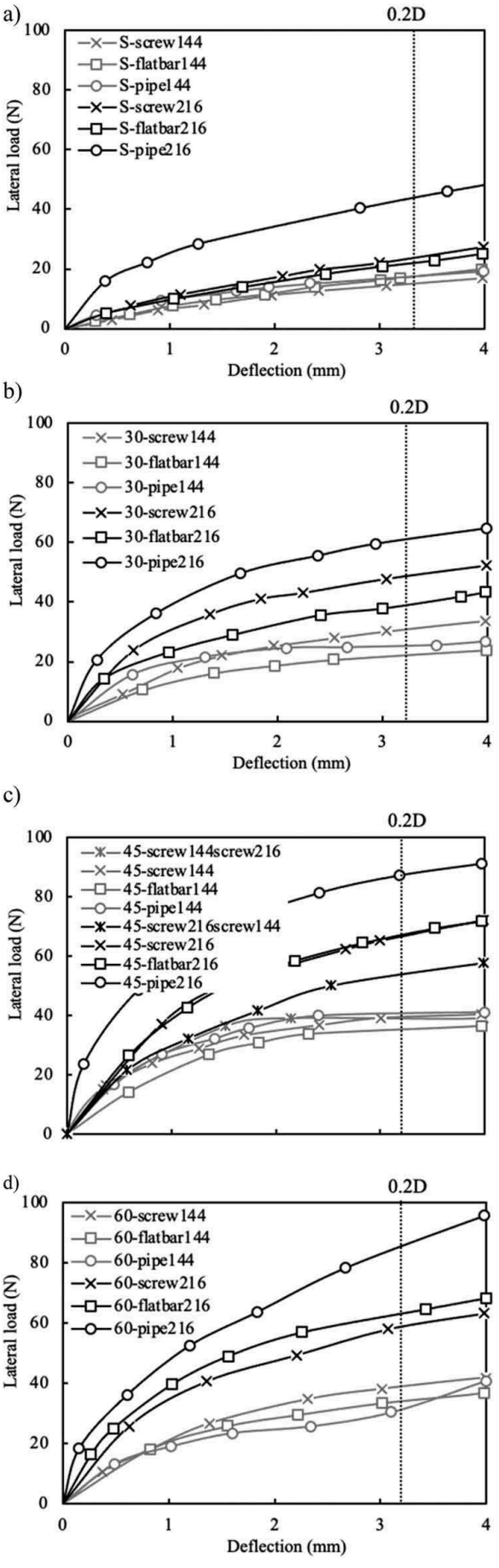

Figure 8. Comparison of ultimate capacity of piles with deflection a) single pile b) 30 degree combination c) 45 degree combination d) 60 degree combination.

defined by the load-deflection curve become linear, and the double tangent method was suggested by Patra & Pise (2001).

However, from the curves in Figure 8, whose results are difficult to be considered as the ultimate lateral capacity, the curves are becoming linear. Therefore, when the 0.2D (or 20% of diameter) deflection is reached, the ultimate lateral capacity could be defined.

Figure 8a shows the results of the ultimate lateral capacity of the single screw, the flat bar, and the pipe

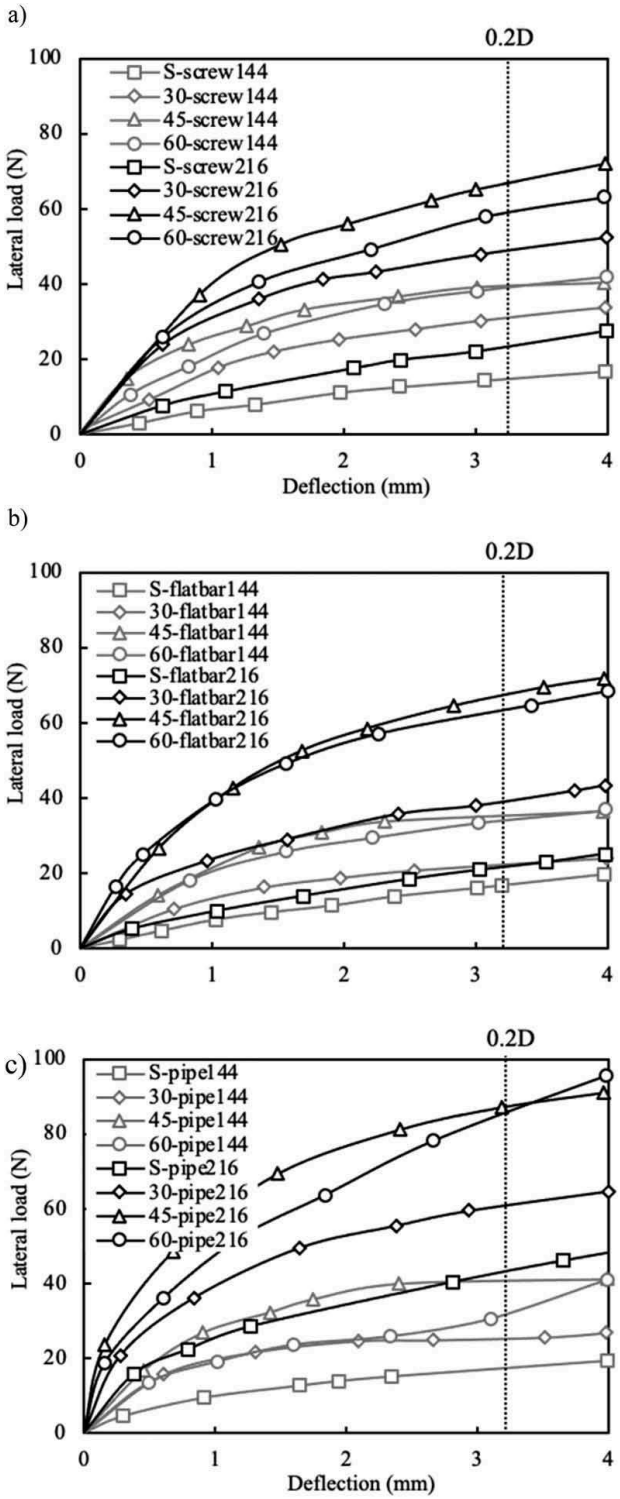

Figure 9. Variation of ultimate lateral capacity with batter angles in case of a) screw b) flat bar c) pipe.

model piles, respectively. The result of a case of 144 mm shows not much difference between screw, flat bar, and pipe. However, in the case of 216 mm, the flat bar and screw pile were shown a similar amount of ultimate lateral capacity aside pipe and can be found an obvious difference between pipe and screw pile (Figure 8).

Results indicated that the ultimate lateral capacity of the screw was decreasing with increasing batter angle. In the case of a 45 degree combination, the screw pile was shown close amount with a flat bar. The pipe pile combination was shown higher ultimate lateral capacity than others (Figure 8b, c, d).

Figure 9 shows the variation of the ultimate lateral capacity of batter angle increment in each type of pile. 45 degree combination indicated the higher value in ultimate lateral capacity in every pile. Meanwhile, the 30 degree combination indicated a lower value in the ultimate lateral capacity, as shown in Figure 10.

In Figure 11, the normalized ultimate lateral capacity was evaluated using the ratio of the ultimate lateral capacity of a coupled pile (H_{u_degree}) and the ultimate lateral capacity of a single pile (H_{u_single}). Screw configuration showed a higher value than that of the flat bar and the pipe, which indicates that the screw pile has a more efficient working ability in lateral loading with reinforcement batter piles than others. However, in the case of the 216 mm pile, the normalized value of the flat bar was increased in the case of 45 and 60 degrees dramatically.

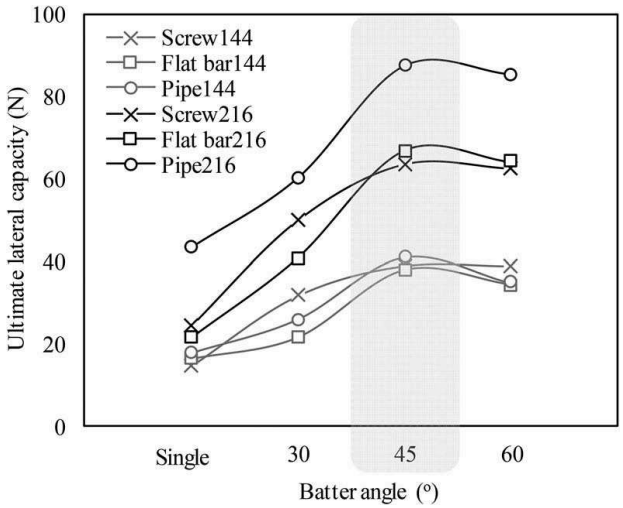

Figure 10. The ultimate lateral capacity with batter angle.

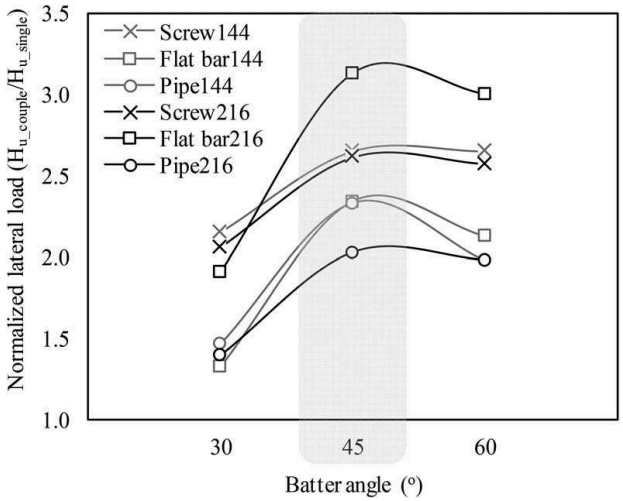

Figure 11. Variation of the normalized ultimate lateral capacity and the ultimate lateral capacity in different angles.

4 CONCLUSIONS

The aim for research on the screw pile with the batter pile behavior comparing with other conventional types of pile foundation under lateral loading is addressed by conducting experiments on model piles. Soil medium was selected as sand, which is used as a dense state. Dimensions of the pile were modeled carefully, avoiding boundary effects and using proper scaling down for the experimental chamber. Experiments were carried out for single piles and coupled piles under lateral monotonic loading to investigate the effect of the screw to find out the proper angle in combined piles. The pile capacities under lateral loading were interpreted from the experiments. The pile head displacement/deflection during lateral monotonic was also measured and analyzed in this study. From the test results, the following conclusions can be drawn:

- The bending moment in single piles was shown relatively higher than the vertical pile in coupled piles. After reinforcing with batter piles as 30, 45, 60 degrees, the bending moments of the vertical pile in the screw, flat bar, and pipe were transferred to batter piles. Bending moments in the model piles showed the nearly same pattern in the bending moment along with the pile depth aside from the case of the 216 mm pile. The maximum bending moments in configurations were measured at the same depth as 62 mm in 144 mm and 92 mm in 216 mm, respectively.
- The model piles showed close values comparing with each other in a single case aside from the case of pipe in the 216 mm pile. The screw pile showed slightly less ultimate lateral capacity than the other two. The ultimate lateral capacity of 216 mm of single screw pile was shown 1.5 times higher value than 144mm pile.
- Results indicated that the ultimate lateral capacity of the screw was decreasing with increasing batter angle. In the case of a 45 degree combination, the screw pile was shown close amount with a flat bar. Meanwhile, the pipe pile combination was shown a higher ultimate lateral capacity than others.
- The normalized ultimate lateral capacity of screw configuration showed a higher value than a flat bar and the pipe, which indicates that the screw pile has the more efficient working ability in

lateral loading with reinforcement batter piles than others. However, in the case of 216 mm of the pile, the normalized value of the flat bar was increased in the case of 45degrees degree dramatically.

ACKNOWLEDGMENTS

The authors would like to thank Mr. Michio Nakajima, Technician of Geotechnical Engineering Laboratory, Kyushu University, for providing technical support in this research.

REFERENCES

Amarbayar, J., Yasufuku N., Ishikura, R., Tani, Y., Nagata, M. & Kurokawa, T. 2020. Experimental studies on the behavior of screw vertical-batter pile under lateral loading in the sand. *The 55th Geotechnical Research Presentation*.

Chandrasekaran, S. S., A. Boominathan, & G. R. Dodagoudar. 2010. Group interaction effects on laterally loaded piles in clay. *J. Geotech. Geoenviron. Eng*. 136 (4): 573–582.

Georgiadis, K & Georgiadis, M. 2010. Undrained lateral pile response in sloping ground. *J. Geotech. Geoenviron. Eng*: 1489–1500

Hirata, A., Kokaji, S., Kang, S, S. & Goto, T. 2005. Study on the Estimation of Axial Resistance of Spiral Bar Based on Interaction with Ground. *Shigen-to-Sozai*, 121. 8. (in Japanese) (submitted).

Kurokawa, T., Tani, Y., Nagata, M. & Nagasaki, R. 2020. Tension and Four-Point Bending Test of Spiral Piles (Twisting a Strip Flat Steel). *The 55th Geotechnical Research Presentation, online* (in Japanese).

Lee, J., Kim, M & Kyung, D. 2010. Estimation of lateral load capacity of rigid short piles in sands using CPT result. *J. Geotech. Geoenviron. Eng*: 48–56.

Meyerhof, G. G. 1981. The bearing capacity of rigid piles and pile groups under inclined load in clay. *Can. Geotech. J*: 18(2). 159–170.

Narasimha Rao, S., V. G. S. T. Ramakrishna, & M. Babu Rao. 1998. Influence of rigidity on laterally loaded pile groups in marine clay. *J. Geotech. Geo-environ. Eng*. 124 (6): 542–549.

Patra, N. R & Pise, P. J. 2001. Ultimate lateral resistance of pile groups in the sand. *J. Geotech. Geoenviron. Eng*: 481–487.

Rao, S. N & Prasad, Y. V. S. N. 1993. Uplift behavior of pile anchors subjected to lateral cyclic loading. *J. Geotech. Eng*: 786–790.

Sato, T., Harada, T., Iwasa, N., Hayashi, S. & Otani, J. 2010. Effect of shaft rotation of spiral piles under its installation on vertical bearing capacity. *Japanese Geotechnical Journal*, 10. 2. 253–265.

Tani, Y., Wang, K., Yasufuku N., Ishikura, R., Fujimoto, H. & Nagata, M. 2019. Model test for bearing capacity of the spiral pile in sandy ground focused on pitch-width ratio. *The 54th Geotechnical Research Presentation, Saitama (in Japanese) (submitted*).

Tani, Y., Amarbayar, J., Yasufuku N., Ishikura, R., Kurokawa, T. & Nagata, M. 2020. Horizontal Loading Test of Spiral Piles in Sand. *The 55th Geotechnical Research Presentation, online (in Japanese*).

Wang, K., Tani, Y., Yasufuku N., Ishikura, R., Fujimoto, H. & Nagata, M. 2019. Bearing capacity characteristics of the spiral pile in sandy ground focused on pitch-width ratio. *The 54th Geotechnical Research Presentation, Saitama*.

Wood, D. M. 2004. *Geotechnical modeling*. New-York: Spon Press, Taylor & Francis Group.

Wood. D. M., Crewe, A., & Taylor, C. 2002. Shaking table testing of geotechnical models. *Int. J. Phys. Model. Geotech*: 2(1). 1–13.